Doppler-free spectroscopy of the 5882-Å line of ^{20}Ne I*

Salim N. Jabr† and W. R. Bennett, Jr.
Dunham Laboratory, Yale University, New Haven, Connecticut 06520
(Received 30 July 1979)

An experimental study of pressure broadening and shifts on the 5882-Å line of Ne I was conducted with a resolution of one part per billion by means of saturation spectroscopy with a zero-pressure reference line provided by a metastable-atomic-beam apparatus. A broadening of 11 ± 2 MHz per Torr was found for Ne-Ne collisions and an upper limit of 500 kHz per Torr was found for the shift. The cross section for large-angle Ne*-Ne scattering was found to be 46 ± 4 Å^2 from collisional cross-relaxation effects. A theory was developed to account for line-shape distortion effects in saturation spectroscopy with optically thick samples.

INTRODUCTION

The sharpness of the laser spectrum[1] and the spectral hole-burning process[2] are the two primary phenomena that have so far permitted extending single-quantum, tuned-laser spectroscopy to below the Doppler-broadened level. The range of tunability in even the earliest gas lasers permitted use of the Lamb dip[3] and other hole-burning effects to measure isotope shifts within the Doppler width in gas discharges.[4] The use of intracavity inhomogeneously broadened "nonlinear" absorbers permitted the observation of similar but inverted tuning dips at much lower pressure and hence with small pressure-broadened Lorentz widths.[5] The direct observation of isolated hole-burning effects in external cells[6] was followed by the investigation of a series of external standing-wave resonance effects,[7] which are of a simpler and different nature than the Lamb dip and which are capable of greater resolution. Most of these experiments involve burning a hole on one side of the velocity distribution with a strong running wave and probing the tail of the resultant gain or absorption hole on the other side of the line using a running wave traveling in a direction opposite to the first and of the same frequency. Of the various techniques developed, the particular phase-sensitive detection method in which only the strong wave is modulated and the oppositely directed probing wave is detected[8] has enjoyed widest use. This method is, in fact, so popular that many people have come to regard the technique itself as "saturation spectroscopy," and it is the primary method used in the present research. A second, well-known technique for Doppler-free single-photon spectroscopy incorporated in the present research involves the use of crossed atomic and laser beams. In our case, a well-collimated beam of metastable atoms was crossed at right angles with a tunable single-frequency laser. When the laser is swept through a resonance to excite an upper level, a decrease in detected beam current occurs. The method is the same as that used recently by Wik *et al.*[9] in the measurement of isotope shifts in neon and is analogous to the well-known atomic beam resonance experiment by Lamb and Retherford.[10] (A more detailed discussion of spectral hole-burning effects was given by Bennett in Ref. 11, and more general reviews of "saturation" or "nonlinear" spectroscopy were given recently by Chebotayev and Letokhov in Refs. 12 and 13. Jacquinot has also provided a recent survey of atomic-beam–laser spectroscopy experiments in Ref. 14.) In the present paper we report the application of these two methods to the study of pressure shifts and line broadening on the 5881.89-Å (air) transition of Ne I from the $1s_5$ metastable to the short-lived $2p_2$ state (see Fig. 1).

THEORY

Collisions between "emitting" and "perturbing" atoms are, of course, the main phenomena around which this study revolves. Line shifts and broad-

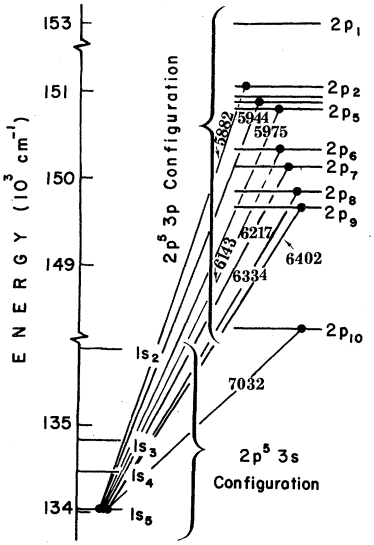

FIG. 1. Relevant energy levels in neon.

ening as well as the redistribution of saturation over the whole Doppler-broadened spectroscopic line are all collisional perturbations of the atom-field interaction that causes line shift and pressure broadening, whereas the velocity-changing aspect of collisions causes the redistribution of saturation over the Doppler line. This phenomenon is generally referred to as "collisional cross relaxation." There is another mechanism which leads to cross relaxation: namely, radiation trapping on resonance transitions studied by Beterov *et al.*[15] However, the present work deals only with states that are not optically connected with the atomic ground state and for which trapping of resonance radiation does not occur.

A number of authors have given detailed theoretical accounts of collisional cross relaxation using the density-matrix formalism (e.g., see the papers by Rautian, Berman, and Lamb in Refs. 16–18). However, most of these papers make approximations, such as the assumption of equal upper- and lower-state lifetimes, which are inapplicable to the present experiment. Berman has recently given a general review of the study of collisions by laser spectroscopy.[19] We shall adapt the initial treatment of cross relaxation by Smith and Hänsch (see Ref. 8) to apply to the present case.

We start with the rate equations describing the evolution of the upper- and lower-state population densities $n_2(v)$ and $n_1(v)$,

$$\frac{\partial n_i(v)}{\partial t} = F_i(v) - \gamma_i n_i(v) - I\sigma(v)[n_i(v) - n_j(v)], \qquad (i,j) = (1,2) \text{ or } (2,1), \quad (1)$$

in the presence of an electromagnetic field with electric vector

$$E = E_0 \sin(wt - \vec{k}\cdot\vec{z}). \qquad (2)$$

The densities are considered to be functions of the velocity in the direction of propagation of the field with intensity I. The stimulated transition rate per unit intensity is given by[11]

$$\sigma(v) = \frac{8\pi}{\hbar^2 c} \frac{(\gamma_0 \langle 1 \mid \mu \mid 2\rangle^2)}{[\gamma^2 + 4(\omega_{12} - \omega - \vec{k}\cdot\vec{v})^2]},$$

where

$$\gamma_0 \equiv R_1 + R_2, \quad \gamma \equiv \gamma_0(1+S)^{1/2}$$

are the natural and power-broadened linewidths (FWHM). R_i is the total phase interruption rate for level i ($i = 1, 2$), and

$$S = (8/c\hbar^2)\langle 1 \mid \mu \mid 2\rangle^2 I/R_1 R_2$$

is the saturation parameter. The pumping rate $F_i(v)$ of level i is assumed to be Maxwellian in velocity:

$$F_i(v) = F_i f(v), \text{ where } f(v) = (1/\bar{v}\sqrt{\pi}) e^{-v^2/\bar{v}^2}.$$

The constant γ_i is the sum of all decay rates from level i which are not due to electron collisions or stimulated emission, and is quite distinct from the total elastic and inelastic collision rates (γ_0, γ, R_1, and R_2). (See Fig. 2.)

In order to include the effect of redistribution of atoms in level i over velocity space due to elastic collisions we must add to Eq. (1) the collision term

$$\left(\frac{\partial n_i(v)}{\partial t}\right)_{\text{coll}} = -n_i(v) \int \Gamma_i(v', v) dv' + \int n_i(v) \Gamma_i(v, v') dv, \quad i = 1 \text{ or } 2.$$

The kernel $\Gamma_i(v', v)$ is the probability per unit time that an atom will undergo a velocity change from v to v' due to collisions. The functional dependence of Γ_i on v and v' is determined by the nature of the collisions involved. The present experiment deals with Ne-Ne collisions, and we have chosen to describe the scattering with Keilson-Storer-type kernels:

$$\Gamma_i(v', v) = \frac{\Gamma_i}{\bar{v}[\pi(1-x^2)]^{1/2}} \exp\left(-\frac{(\vec{v} - x\vec{v}')^2}{\bar{v}^2(1-x^2)}\right),$$

where the constant x characterizing the collision strength will be taken equal to zero. Thus

$$\Gamma_i(v', v) = \Gamma_i f(v'), \quad f(v') = (1/\bar{v}\sqrt{\pi}) e^{-(v'^2/\bar{v}^2)}. \qquad (3)$$

This specific model implies that the probability for the process $v \to v'$ is independent of the initial velocity $\vec{v}$. Such an assumption is obviously correct when the atoms studied are scattered by much heavier atoms and remains reasonably good when the emitting and scattering atoms are of equal mass (see Ref. 16); Eq. (1) then becomes

$$\frac{\partial n_i}{\partial t} = F_i f(v) - \gamma_i n_i(v) - I\sigma[n_i(v) - n_j(v)] - \Gamma_i n_i(v) + \Gamma_i f(v) \int_{-\infty}^{\infty} n_i(v') dv', \qquad (i,j) = (1,2) \text{ or } (2,1). \quad (4)$$

We are interested in the steady-state solutions; hence we set Eqs. (4) equal to zero (for $i = 1, 2$). The resulting equations can be solved in the limit of large Doppler broadening and small light intensity, yielding

$$\delta[n_i(v) - n_2(v)] = f(v)(N_2^0 - N_1^0) I \times \left[\left(\sigma(v) + \frac{\Gamma_1}{\gamma_1} \int f(v)\sigma(v) dv\right) / (\gamma_1 + \Gamma_1) + (1 \leftarrow 2)\right] \quad (5)$$

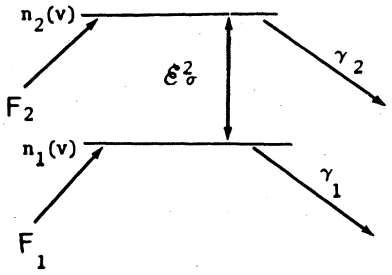

FIG. 2. Generalized two-level system.

for the change in the population difference due to the saturating field. Finally, the change in the absorption coefficient k of the probe beam is given by

$$\delta\kappa = h\nu \int_{-\infty}^{\infty} \sigma_0(v)\,\delta[n_i(v) - n_2(v)]\,dv\,, \tag{6}$$

where

$$\sigma_0(v) \equiv (8/\hbar^2 c)\gamma_0 \langle 1 \,|\, \mu \,|\, 2\rangle^2 / [\gamma_0^2 + 4(\omega_{12}^2 - \omega + \vec{k}\cdot\vec{v})^2]\,.$$

Equation (5) and (6) give

$$\delta\kappa = Ih\nu(N_2^2 - N_1^0)\left(C_1 \int f(v)\sigma\sigma_0\,dv + C_2 \int f(v)\sigma\,dv \int f(v)\sigma_0\,dv\right),$$

where

$$C_1 \equiv \sum_i \frac{1}{\Gamma_i + \gamma_i}\,, \quad C_2 \equiv \sum_i \frac{\Gamma_i/\gamma_i}{\Gamma_i + \gamma_i}\,.$$

The first integration can be carried out exactly in the Doppler-broadened limit and is equal to the product of a Gaussian and a Lorentzian of width (FWHM)

$$\Delta\nu_L = \gamma_p/2\pi = (\gamma_0/4\pi)(1 + \sqrt{1+S})\,. \tag{7}$$

The second term in the large parentheses is the product of two Gaussians of widths equal to the Doppler width. Hence

$$\delta\kappa = AS\kappa_0(v)\left(\frac{2C_1}{(\gamma/2\pi)}\,\mathcal{L}(v) + \frac{C_2}{\Delta\nu_D(16\pi\ln 2)^{1/2}}\,\mathcal{G}(\nu)\right), \tag{8}$$

where

$$\kappa_0(\nu) = (16\pi\ln 2)^{1/2}(N_2^0 - N_1^0)\langle\mu_{12}\rangle^2 \frac{2\pi\nu}{ch\Delta\nu_D}\,\mathcal{G}(\nu)\,,$$

$$\mathcal{G}(\nu) \equiv \exp\{-[(\nu - \nu_0)/\Delta\nu_D]^2 4\ln 2\}\,,$$

$$\mathcal{L}(\nu) \equiv 1/\{1 + 4\pi^2[(\nu - \nu_0)/\gamma_{p/2}]^2\}\,,$$

S is the saturation parameter, and

$$A \equiv R_1 R_2/(4\ln 2)^{1/2}\,.$$

It is seen from Eq. (8) that the change in the absorption coefficient has a narrow Lorentzian part at line center and a broad Gaussian part due to cross relaxation. The ratio of the amplitude of the Gaussian part to the Lorentzian part is

$$\chi = (4\pi\ln 2)^{1/2}(\gamma_p/2\pi\Delta\nu_D)C_2/C_1\,. \tag{9}$$

For the $1s_5 - 2p_2$ transition in Ne I we have $\gamma_2 \gg \gamma_1$ and we obtain

$$\chi = (4\pi\ln 2)^{1/2}(\gamma_p/2\pi\Delta\nu_D)\Gamma_1/\gamma_1\,. \tag{10}$$

In most saturated absorption spectroscopy experiments, one really observes the change of the intensity of the probe beam and not the absorption coefficient. When the optical thickness is large, substantial distortion in the resonance line shape occurs. This distortion of the Gaussian part of the signal comes from the frequency-dependent decrease of the saturation beam intensity as it propagates through the cell. Such an effect has not been reported in the literature to our knowledge. The effect becomes very pronounced as soon as the optical thickness kL exceeds a value of 2 (L is the cell length).

Assuming a simple exponential decay for the saturating beam intensity and integrating the propagation equation $di/dz = -k_S(\nu)i$ for the weak beam over the cell length, we obtain the following expression for the observed signal (i.e., the change in the weak beam intensity due to the saturating beam):

$$\Psi(\nu, S_i, \kappa_0 L) = \exp[-\kappa_0 L + \kappa_0 A(\mathcal{L} + \chi\,\mathcal{G})(S_f\kappa_0 L + \Phi)] - \exp(-\kappa_0 L)\,. \tag{11}$$

Here, S_f is the value of the saturation parameter at the cell exit and Φ is given by

$$\Phi = (1 - u_f^2)\ln B + u_f^2(\tfrac{4}{3}u_f - u_i) + \tfrac{2}{3}u_i^3 + 2(u_f - u_i)\,,$$

where

$$B \equiv (u_f - 1)(u_i + 1)/(u_f + 1)(u_i - 1)\,,$$

$$u_i \equiv (1 + S_i)^{1/2}, \quad u_f \equiv (1 + S_f)^{1/2}\,.$$

A computer program to calculate and plot this expression as a function of the detuning was written. The program starts at some value of the detuning and, given values for kL and S_i, calculates S_f and Ψ, plots a point, and proceeds to the next value of the detuning frequency. Results of these numerical calculations are shown in Fig. 3, where the computed values have been fitted to actual experimental data for increasing values of the absorption parameter.

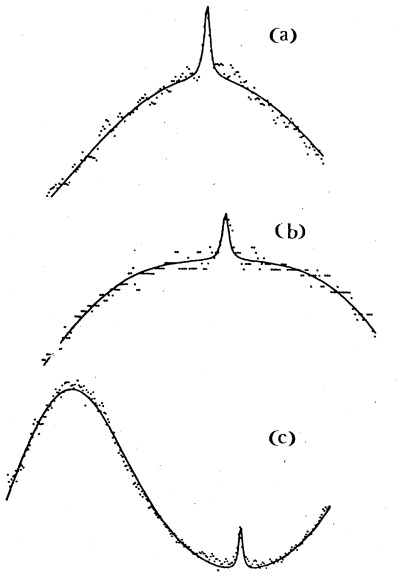

FIG. 3. Saturation signal as a function of increasing optical thickness [increases (a) through (b)].

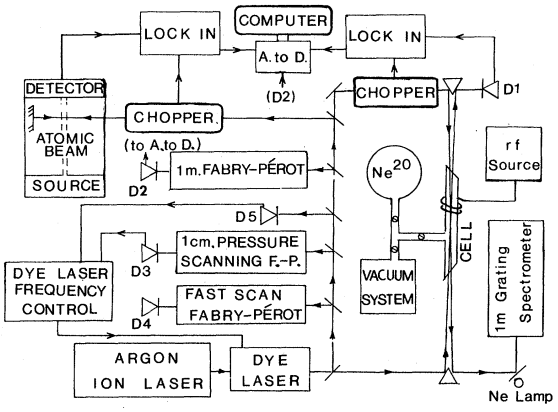

FIG. 4. Schematic diagram of the experimental apparatus. D1 through D5 are photodiodes. Solid arrows indicate the light path; open arrows are electronic circuit paths.

EXPERIMENTAL METHOD

Radiation from a single-mode narrow-band tunable dye laser was simultaneously fed to a metastable-atomic-beam apparatus, a saturation spectrometer and a stable reference Fabry-Perot interferometer of known free spectral range (see Fig. 4). The saturation spectroscopy technique described above provides the resolution required for the experiment as well as valuable information about collisional broadening and cross-relaxation effects. The metastable-atomic-beam apparatus provides nearly ideal conditions for the observation of an atomic line free from the perturbing effects of collisions, electrons in the discharge, and stray electric fields. Finally, the frequency scale is obtained by observing the transmission peaks of the stable Fabry-Perot of known plate separation. We have also used a modification of the arrangement shown in Fig. 4 in which the atomic beam reference was replaced by a second saturable absorber cell operated at different pressures from the first. The general experimental procedure remains the same in that case, except that instead of comparing the signals from the atomic beam apparatus with those from a saturation cell, one compares the signals from two saturation cells at different pressures.

The saturation spectrometer, composed of an absorption cell, gas handling system, rf generator, and signal detection apparatus, is shown on the right-hand side of Fig. 4. The atomic beam machine and associated detection equipment are shown in the upper left corner. D1–D5 are photodetectors. The dye laser, argon-ion pump laser, and Fabry-Perot interferometers used to control and measure the laser frequency are shown in the lower central part.

The laser frequency was locked by an active feedback loop to the side of a transmission peak of a pressure-scannable Fabry-Perot interferometer. A very linear scan of the laser frequency was then obtained by admitting nitrogen to the controlling Fabry-Perot through a slow leak from a high-pressure tank. Although it never exceeded 1 psi, this increase in nitrogen pressure provided a sufficient change in refractive index to scan the transmission and laser frequency through several GHz. The sweep nonlinearity that was obtained in this manner was less than 1 part in 1500. A 1-m Jarrel-Ash grating spectrometer and Ne Geissler tube were used to tune the laser to the desired line. The neon metastable flux in the atomic beam, the intensity of the probe laser beam passing through the absorption cell, and the transmission of the stable reference laser were all recorded simultaneously as the dye-laser frequency was scanned through the atomic line. All three signals went into a multichannel analog-to-digital converter which took data at preset intervals controlled by a computer. As well as storing the data, the computer permitted fitting the points to prescribed theoretical expressions by means of the method of least squares.

Figure 5 shows the result of the fitting procedure applied to the transmission resonances from the stable reference Fabry-Perot. The length of this Fabry-Perot gave fringes spaced by 158.89 MHz, thus providing the frequency scale for our

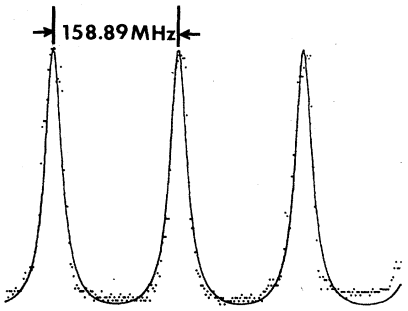

FIG. 5. Transmission fringes from the reference Fabry-Perot interferometer.

other measurements.

Figure 6 shows data for the atomic beam resonance fit to a Lorentzian response function. Here, the linewidth arises primarily from power broadening. For these measurements, the laser beam was reflected back on itself to avoid any possible systematic shifts of the line center due to residual first-order Doppler effect. Laser frequency jitter introduced about 2 MHz of additional broadening and the metastable atomic beam divergence added another 5 MHz to the width of the resonance. The curve in Fig. 7 shows data for the saturation signal fitted to Eq. (11). Only a small part of the large Doppler background is shown here because of the limited range of the scan [c.f. Fig. 3(a)].

RESULTS

Table I shows some results for the pressure shift of the $3s\,^3P_2^o \rightarrow 3p\,^3P_1$ transition of Ne I ($1s_5 \rightarrow 2p_2$ in Paschen notation) in neon-neon collisions. The data were taken with ^{20}Ne samples of 99.999% isotoptic purity. An upper limit of 300 kHz/Torr can be put on the pressure-shift coefficient from our data.

Figure 8 shows results obtained with the two-

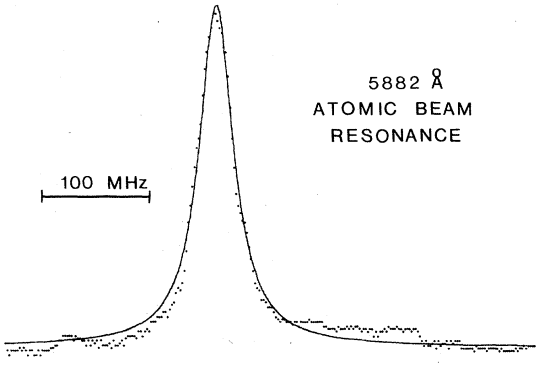

FIG. 6. Least-squares fit of atomic beam resonance to a Lorentzian.

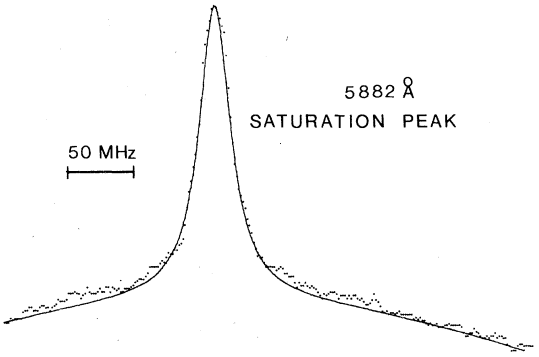

FIG. 7. Least-squares fit of saturation signal to Eq. (11).

cell version of the experiment. The low-pressure cell was kept at 20 mTorr while the pressure in the second cell was varied over the range from 10 to 800 mTorr. The upper limit on pressure in the second cell was determined in practice by collisional cross-relaxation effects. Indeed, the ratio of the Gaussian to Lorentzian components of the signal increased as the square of the pressure as shown in Fig. 9. This quadratic increase is predicted by Eq. (10) because the lifetime of the lower (metastable) state is determined by diffusion of the atoms through the laser beam. When such diffusion is taken into account, the actual decay rate of the lower state varies as the reciprocal of the pressure for pressures higher than about 20 mTorr. From the data in Fig. 9, the Ne-Ne* collision rate can be determined as a function of pressure and is as shown in Fig. 10.

The collision rate in Fig. 10 corresponds to a large-angle Ne-Ne* scattering cross section of 46 ± 4 Å^2 and is consistent with the diffusion coef-

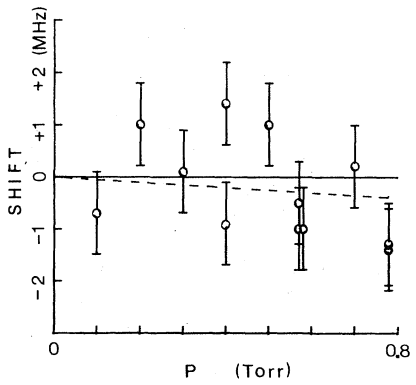

FIG. 8. Shift between the two saturation cells as a function of the pressure in the second cell (first cell at 20 mTorr).

TABLE I. Pressure shift of the $3s^3p_2^o \leftrightarrow 3p\ ^3P_1$ transition in ^{20}Ne.

Cell pressure (mTorr)	Direction of scan [a]	Saturation dip frequency [b] (MHz)	Beam signal center frequency [b] (MHz)	Shift ^{f}cell $-^f$beam (MHz)	Standard deviation
140	+	107.78	108.4	−0.6	0.6
140	+	202.99	202.24	+0.7	0.6
140	−	125.08	125.65	−0.5	0.8
140	−	149.98	149.93	0	0.3
140	+	122.70	122.36	+0.3	0.4
140	+	100.44	100.80	−0.4	0.5
140	−	169.56	169.85	−0.3	0.4
		Average shift (140 mTorr) = −100 ± 200 KHz			
50	+	59.6	59.7	−0.1	0.3
50	+	173.2	172.8	0.4	0.5
50	−	132.5	132.1	0.4	0.5
50	−	98.3	98.6	−0.3	0.5
		Average shift (50mTorr) = 100 ± 300 KHz			
500	+	150.4	150.7	−0.3	0.6
500	+	163.2	163.2	0	0.5
500	−	109.8	110.0	−0.2	0.5
500	−	212.6	212.0	+0.6	0.6
500	+	124.7	124.0	+0.7	0.6
		Average shift (500 mTorr) = 160 ± 250 KHz			

[a] + corresponds to a scan towards higher frequency, and − towards lower frequency.
[b] Relative to start of scan.

ficient for neon metastables determined by Phelps.[20] We should mention that this measurement includes the effects of both metastable exchange and large-angle elastic collisions. The cross section for metastable exchange was measured by Pinard and Leduc,[21] who report a value of 22 ± 6 Å^2 for Ne-Ne*($^3P_2$).

Figure 11 shows a dependence of linewidth on pressure peculiar to transitions involving a metastable lower state. It should be noted that the saturation peak width decreases first with increasing pressures, reaches a minimum at a

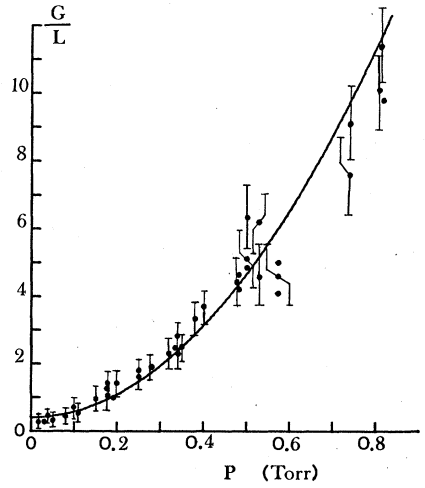

FIG. 9. Pressure dependence of the ratio of the Gaussian to the Lorentzian portions of the saturation signal.

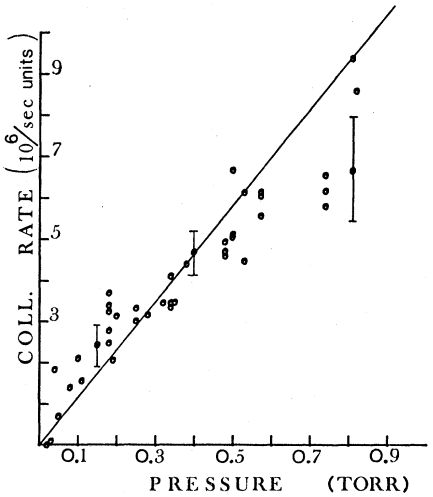

FIG. 10. Ne-Ne* collision rate as a function of pressure.

TABLE II. Broadening and shift in NeI in MHz/Torr. B = broadening; S = shift.

$L\,S$	S_0	$^3P_1$	$^3P_0$	$^3P_2$	$^1P_1$	$^1D_2$	$^3D_1$	$^3D_2$	$^3S_1$
Racah	$3p'[\frac{1}{2}]_0$	$3p'[\frac{1}{2}]_1$	$3p[\frac{1}{2}]_0$	$3p'[\frac{3}{2}]_2$	$3p'[\frac{3}{2}]_1$	$3p[\frac{3}{2}]_2$	$3p[\frac{3}{2}]_1$	$3p[\frac{5}{2}]_2$	$3p[\frac{1}{2}]_1$
Paschen	$2p_1$	$2p_2$	$2p_3$	$2p_4$	$2p_5$	$2p_6$	$2p_7$	$2p_8$	$2p_{10}$
$^1P_1^0$	$B^{i}=40\pm7^{a}$	$B=40\pm5^{a}$		$B=61\pm3^{d}$		$B=61\pm3^{d}$			
	61 ± 1^{d}								
$3s'[\frac{1}{2}]_1^0$	$S^{j}<1^{k}$			$S<1^{d}$		$S<1^{d}$			
$1s_2$	6599 Å			6678 Å		6930 Å			
$^1P_0^0$					$B<5^{a}$		$B=5.3\pm0.3^{d}$		
$3s'[\frac{1}{2}]_0^0$									
$1s_3$					6266 Å		6532 Å		
$^3P_1$		$B<5^{a}$		$B=7.8\pm0.3^{d}$		$B=7.1\pm0.3^{d}$	$B=6.1\pm0.3^{d}$	$B=7.6\pm0.3^{d}$	
$3s[\frac{3}{2}]_1^0$				$S=-2^{d}$		$S=-2^{d}$	$S=-2^{d}$	$S=-2^{d}$	
$1s_4$		6030 Å		6096 Å		6306 Å	6382 Å	6506 Å	
$^3P_2$		$B(300°)=13.5^{d}$		$B=9\pm0.5^{d}$			$B<5^{a}$		
		$S=-2^{d}$							
$3s[\frac{3}{2}]_2^0$		$B=11\pm2^{h}$		$S=-2^{d}$					
		$S=0^{h}$							
$1s_5$		5882 Å		5945 Å			6217 Å		
				$B=8\pm1^{a}$					
				$S<0.2^{e}$					
$4s'[\frac{1}{2}]_1^0$									
$2s_2$				11 520 Å					
				$B=24^{a},25^{b}$ $15^{c},94^{g}$		$B=78\pm12^{g}$	$B=106\pm10^{g}$		$B=34^{a},45^{a},81^{g}$
$5s'[\frac{1}{2}]_1^0$				$S=-6\pm2^{c}$					
$3s_2$			5939 Å	6328 Å		6118 Å	6046 Å		5434 Å

TABLE II. (*Continued.*)

$L\,S$	S_0	$^3P_1$	$^3P_0$	$^3P_2$	$^1P_1$	$^1D_2$	$^3D_1$	$^3D_2$	$^3S_1$
Racah	$3p'[\frac{1}{2}]_0$	$3p'[\frac{1}{2}]_1$	$3p[\frac{1}{2}]_0$	$3p'[\frac{3}{2}]_2$	$3p'[\frac{3}{2}]_1$	$3p[\frac{3}{2}]_2$	$3p[\frac{3}{2}]_1$	$3p[\frac{5}{2}]_2$	$3p[\frac{1}{2}]_1$
Paschen	$2p_1$	$2p_2$	$2p_3$	$2p_4$	$2p_5$	$2p_6$	$2p_7$	$2p_8$	$2p_{10}$
		$B=80\pm7$[g]							
$6s'[\frac{1}{2}]_1^0$		5439 Å							
$4s_2$									
							$B=105\pm35$[2]		
$7s[\frac{3}{2}]_1^0$									
$5s_4$							4892 Å		
				$B=43\pm7$[f]					
$7d'[\frac{5}{2}]_3^0$				$S=-8\pm3$[f]					
$7s_1''''$				4628 Å					
					$B=41\pm7$[f]				
$7d'[\frac{5}{2}]_2^0$					$S=-8\pm4$[f]				
$7s_1''''$					4609.8 Å				
	$B=42\pm8$[f]								
$7d'[\frac{3}{2}]_2^0$	$S=10\pm4$[f]								
$7s_1''$	4667.3 Å								

[a] Reference 26.
[b] Reference 25.
[c] Reference 23.
[d] Reference 22.
[e] Reference 24.
[f] Reference 28.
[g] Reference 27.
[h] This work.

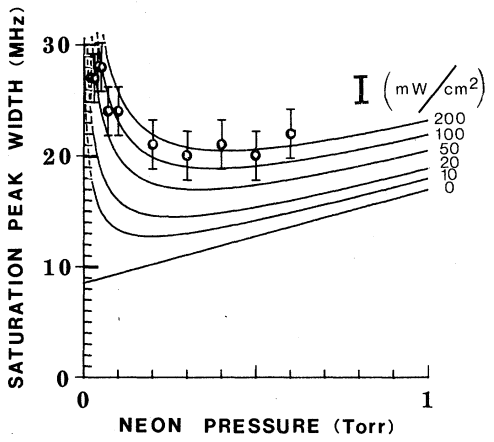

FIG. 11. Saturation peak width as a function of pressure (5882 Å).

pressure determined by the amount of saturation, and then increases with pressure. This behavior results from the dependence of the saturation intensity on pressure via the lower-state relaxation rate. The plotted curves in Fig. 11 correspond to the expression

$$\gamma = \tfrac{1}{2}\gamma_0(1+\beta p)\left[1+\left(1+\frac{3I}{4[3.3cP+1/(1+3cP)]}\right)^{1/2}\right],$$

which follows from Eq. (7). P is the pressure in Torr.

CONCLUSION

Table II summarizes various measurements of the pressure-broadening coefficients for different transitions in atomic neon. The only other measurements besides ours for the broadening of the 5882-Å line are those of Kuhn and Lewis performed at 80°K in Ref. 22. They measured a broadening of 9.6 ± 1 MHz/Torr at 89°K and a shift of 2 MHz/Torr towards the red. Their broadening data agree with our 11 ± 2-MHz/Torr result when the temperature dependence is taken into account. The temperature dependence of the shift is more difficult to take into account since it depends on the specific model used to describe the atomic interaction. The Hindmarsch theory predicts a shift which can go from red to blue as a function of the temperature. However, this theory utilizes the classical trajectory approximation which fails when the scattering from the upper and lower state of the transition is different and the atom enters the collision in a mixed state in the laser field.[17]

ACKNOWLEDGMENTS

The authors are indebted to W. Lichten for the loan of his atomic beam machine and his help in aligning it.

---

*A report of this work was given at the Sixth Vavilov Conference on Nonlinear Optics (USSR, Novosibirsk, June 1979; Invited Paper).

†Present address: Physics Dept., Seaver Science Center, Room 107, University of Southern California, Los Angeles, CA 90007.

[1]A. L. Schawlow and C. H. Townes, Phys. Rev. 112, 1940 (1958); A. Javan, W. R. Bennett, Jr., and D. R. Herriott, Phys. Rev. Lett. 6, 106 (1961).

[2]W. R. Bennett, Jr., Phys. Rev. 126, 580 (1962); Appl. Opt. Suppl. 1, 24 (1962); also see *Quantum Electronics III-Paris 1963 Conference*, edited by P. Grivet and N. Bloembergen (Columbia University, New York, 1964), Vol. I, pp. 441–458.

[3]W. E. Lamb, Jr., Phys. Rev. 134, A1429 (1964); R. A. McFarlane, W. R. Bennett, Jr., and W. E. Lamb, Jr., Appl. Phys. Lett. 2, 189 (1963).

[4]A. Szöke and A. Javan, Phys. Rev. Lett. 10, 521 (1963); also see R. H. Cordover, T. S. Jaseja, and A. Javan, Appl. Phys. Lett. 7, 322 (1965); R. H. Cordover, P. A. Bonczyk, and A. Javan, Phys. Rev. Lett. 18, 730 (1967).

[5]P. H. Lee and M. L. Skolnick, Appl. Phys. Lett. 10, 303 (1967); V. S. Letokhov, Sov. Phys. JETP Lett. 6, 101 (1967); V. N. Lisitsyn and V. P. Chebotayev, Sov. Phys. JETP 27, 229 (1968); R. L. Barger and J. L. Hall, Phys. Rev. Lett. 22, 4 (1969); W. R. Bennett, Jr., Comments At. Mol. Phys. 2, 10 (1970).

[6]W. R. Bennett, Jr., V. P. Chebotayev, and J. W. Knutson, Jr., in *Proceedings of the Fifth International Conference on the Physics of Electronic and Atomic Collisions, Leningrad, 1967*, edited by I. P. Flaks (Nauka, Leningrad, 1967), p. 521; data reproduced in W. R. Bennett, Jr., in *Atomic Physics*, edited by V. W. Hughes, B. Bederson, C. W. Cohen, and F. M. Pichanik (Plenum, New York, 1969), pp. 452–455; C. V. Shank and S. E. Schwarz, Appl. Phys. 13, 113 (1968); T. Hänsch and P. Toschek, IEEE J. Quantum Electron. QE-4, 467 (1968).

[7]P. Rabinowitz, R. Keller, and J. T. LaTourrette, Appl. Phys. Lett. 14, 376 (1969); F. Shimizu, *ibid.* 14, 378 (1969); N. G. Basov, I. N. Kompanetz, O. N. Kompanetz, V. S. Letokhov, and V. V. Nikitin, Sov. Phys. JETP 9, 568 (1969); Yu. A. Matyugin, B. I. Troshin, and V. P. Chebotayev, Opt. Spectrosc. 31, 111 (1971).

[8]C. Bordé, C. R. Acad. Sci. 271, 371 (1970); P. W. Smith and T. Hänsch, Phys. Rev. Lett. 26, 740 (1971).

[9]T. Wik, W. R. Bennett, Jr., and W. Lichten, Phys. Rev. Lett. 40, 1080 (1978).

[10]W. E. Lamb, Jr. and R. C. Retherford, Phys. Rev. 79, 549 (1950).

[11]W. R. Bennett, Jr. in *Atomic Physics and Astrophysics*, edited by M. Chretien and E. Lipworth (Gordon and Breach, New York 1973), Vol. 2, pp. 1–201; and *The*

Physics of Gas Lasers, Documents on Modern Physics Series (Gordon and Breach, New York, 1977).
[12]V. P. Chebotayev and V. S. Letokhov, Prog. Quantum Electron. 4 (2), 111 (1975); also see the articles by these two authors in *High Resolution Spectroscopy*, edited by K. Shimoda (Springer-Verlag, New York, 1976), Topics in Applied Physics, Vol. 13, pp. 95–171, 201–251.
[13]V. S. Letokhov and V. P. Chebotayev, *Nonlinear Laser Spectroscopy* (Springer-Verlag, New York, 1977).
[14]P. Jacquinot in *High Resolution Laser Spectroscopy* (Springer-Verlag, New York, 1976), pp. 52–93.
[15]I. M. Beterov, Yu. A. Matyugin, S. G. Rautian, and V. P. Chebotayev, Sov. Phys.–JETP 31, 668 (1970) [Zh. Eksp. Teor. Fiz. 58, 1243 (1970)].
[16]S. G. Rautian, Sov. Phys. JETP 24, 788 (1967).
[17]P. R. Berman and W. E. Lamb, Jr., Phys. Rev. A 2, 2435 (1970).
[18]P. R. Berman, Appl. Phys. 6, 283 (1975).
[19]P. R. Berman, Adv. At. Mol. Phys. 13, 62 (1977).
[20]A. V. Phelps, Phys. Rev. 114, 1011 (1959).
[21]M. Pinard and M. Leduc, J. Phys. (Paris) 38, 609 (1977).
[22]H. G. Kuhn and E. L. Lewis, Proc. R. Soc. London 299, 423 (1967).
[23]V. N. Lisitsyn and V. P. Chebotayev, Sov. Phys. JETP 27, 227 (1968).
[24]J. L. Hall, IEEE J. Quantum Electron. QE-4, 638 (1968).
[25]P. W. Smith and T. Hänsch, Phys. Rev. Lett. 26, 740 (1971).
[26]Yu. A. Matyugin, A. S. Provorov, and V. P. Chebotayev, Sov. Phys. JETP 36, 1080 (1972).
[27]J. W. Knutson, Jr. and W. R. Bennett, Jr., Phys. Rev. A 13, 318 (1978).
[28]M. M. Salour, Ph.D. thesis, Harvard University, 1977 (unpublished); Ann. Phys. (to be published).